Supporting Information

Stein and Alexandrov 10.1073/pnas.1405220111

SI Materials and Methods

Cloning Procedures.

General. Single-stranded oligonucleotides and gBlock DNA fragments were obtained commercially from Integrated DNA Technologies. Melting temperatures for PCR reactions were calculated with the Sigma Genosys Oligocalculator. All PCR, restriction enzyme digests, USER Enzyme, and T4 DNA ligase-mediated multifragment DNA assembly reactions were purified using the QIAquick PCR purification kit before use. PCRs were performed according to standard conditions using polymerase PfuX7 (1) with 1 μM forward and reverse primers, 250 nM dNTPs each, 20 mM Tris·HCl (pH 8.8 at 25 °C), 10 mM $(NH_4)_2SO_4$, 10 mM KCl, 100 μg/mL BSA, 0.1% (vol/vol) Triton X-100, and 2 mM $MgSO_4$. Extension times were 30 s/kbp DNA and the melting temperature chosen was 2 °C less than the lesser melting temperature for a particular pair of primers as calculated by the Sigma Genosys Oligocalculator. DNA fragments were constructed according to desired specification with USER Enzyme-T4 DNA ligase-based assembly methods similar to previously published procedures (2, 3) or by Gibson assembly (4) and then inserted into the MBP fusion expression vector 00941 (Fig. S1*A*). This construct is based on a previously developed construct pRK793 for the expression of the NIa protease from Tobacco Etch Virus (TEV) where MBP acts as a molecular chaperone enabling more efficient recombinant expression of NIa proteases in *E. coli* (5). Expression constructs for TVMV and HCV were designed in an analogous fashion and also contained a cleavage site to enable autoproteolytic processing from MBP during expression in vivo. The desired product from USER Enzyme-T4 DNA Ligase assembly reactions was generally purified by agarose gel electrophoresis using the Promega Gel Extraction Kit. For detailed cloning procedures, please contact the authors.

Summary of protein coding sequences. A list of protein-coding sequences of all of the different protease-based biosensors is given below. The amino acid sequence of the protease is underlined, the amino acid sequence of the molecular sensing entity (i.e., either the cleavage site for an activating protease or an affinity clamp) is bold, the amino acid sequence of the autoinhibitory peptide is double-underlined, and the amino sequence coding for SH3-based scaffolding interactions is wave-underlined. The amino acid sequence of FRB and FKBP12 are bold and wave-underlined. The His_6 tag at the C terminus and the connecting linker sequences are in plain font.

$TVMV^{Thr}$-AI. SSGSKALLKGVRDFNPISACVCLLENSSDGHSERLFGIGFGPYIIANQHLFRRNNGELTIKTMHGEFKVKNSTQLQMKPVEGRDIIVIKMAKDFPPFPQKLKFRQPTIKDRVCMVSTNFQQKSVSSLVSESSHIVHKEDTSFWQHWITTKDGQCGSPLVSIIDGNILGIHSLTHTTNGSNYFVEFPEKFVATYLDAADGWCKNWKFNADKISWGSFILWEDAPEDFMSG**LVPRGV**GREYVRFAPGSTHHHHHH

HCV^{TVMV}-AI. SMSTSGSGSGSAKGSVVIVGRINLSGDTAYSQQTRGAAGIAATSATGRDKNQVDGEVQVLSTATQSFLATCVNGVCWTVYHGAGSKTLAGPKGPITQMYTNVDQDLVGWPAPPGARSMTPCTCGSSDLYLVTRHADVIPVRRRGDSRGSLLSPRPVSYLKGSSGGPLLCPSGHVVGIFRAAVCTRGVAKAVDFIPVESMETTMRGGGGSGG**ETVRFQS**GGSGGDELILCPLDLGGSGGTGHHHHHH

$TVMV^{L1}$-PDZ^{L2}-$FN3^{L3}$-AI^{1}. SSGSKALLKGVRDFNPISACVCLLENSSDGHSERLFGIGFGPYIIANQHLFRRNNGELTIKTMHGEFKVKNSTQLQMKPVEGRDIIVIKMAKDFPPFPQKLKFRQPTIKDRVCMVSTNFQQKSVSSLVSESSHIVHKEDTSFWQHWITTKDGQCGSPLVSIIDGNILGIHSLTHTTNGSNYFVEFPEKFVATYLDAADGWCKNWKFNADKISWGSFILW(LINKER_L1)**SPELGFSISGGVGGRGNPFRPDDDGIFVTRVQPEGPASKLLQPGDKIIQANGYSFINIEHGQAVSLLKTFQNTVELIIVREVGNGAKQEIRVRVEKD**(LINKER_L2)**GVSSVPTNLEVVAATPTSLLISWDAYRELPVSYYRITYGETGGNSPVQEFTVPGSKSTATISGLKPGVDYTITVYAHYNYHYYSSPISINYR**(LINKER_L3)REYVRFAPGSTHHHHHH

$SH3$-$TVMV^{E217}$-PDZ^{G38}-$FN3^{GPG}$-AI. SGGSGAEYVRALFDFNGNDEEDLPFKKGDILRIRDKPEEQWWNAEDSEGKRGMIPVPYVEKYRPASASVSALIGGRGGSGGSGGSGGSGGSGGSSKALLKGVRDFNPISACVCLLENSSDGHSERLFGIGFGPYIIANQHLFRRNNGELTIKTMHGEFKVKNSTQLQMKPVEGRDIIVIKMAKDFPPFPQKLKFRQPTIKDRVCMVSTNFQQKSVSSLVSESSHIVHKEDTSFWQHWITTKDGQCGSPLVSIIDGNILGIHSLTHTTNGSNYFVEFPEKFVATYLDAADGWCKNWKFNADKISWGSFILWESG**SPELGFSISGGVGGRGNPFRPDDDGIFVTRVQPEGPASKLLQPGDKIIQANGYSFINIEHGQAVSLLKTFQNTVELIIVREVGNGAKQEIRVRVEKDGGSGGGGVSSVPTNLEVVAATPTSLLISWDAYRELPVSYYRITYGETGGNSPVQEFTVPGSKSTATISGLKPGVDYTITVYAHYNYHYYSSPISINYR**GPGREYVRFAPGSTHHHHHH

HCV^{TVMV}-AI-SH3. SMSTSGSGSGSAKGSVVIVGRINLSGDTAYSQQTRGAAGIAATSATGRDKNQVDGEVQVLSTATQSFLATCVNGVCWTVYHGAGSKTLAGPKGPITQMYTNVDQDLVGWPAPPGARSMTPCTCGSSDLYLVTRHADVIPVRRRGDSRGSLLSPRPVSYLKGSSGGPLLCPSGHVVGIFRAAVCTRGVAKAVDFIPVESMETTMRGGSGGSGGSGG**ETVRFQS**GGSGGDELILCPLDLGGSGGSGGPPPPLPPKRRRGGTGHHHHHH

$FKBP12$-$TVMV^{Thr}$-AI. GGSGGSGG**VQVETISPGDGRTFPKRGQTCVVHYTGMLEDGKKFDSSRDRNKPFKFMLGKQEVIRGWEEGVAQMSVGQRAKLTISPDYAYGATGHPGIIPPHATLVFDVELLKLE**GGSGGSGGSGGSGGSGGSGGSKALLKGVRDFNPISACVCLLENSSDGHSERLFGIGFGPYIIANQHLFRRNNGELTIKTMHGEFKVKNSTQLQMKPVEGRDIIVIKMAKDFPPFPQKLKFRQPTIKDRVCMVSTNFQQKSVSSLVSESSHIVHKEDTSFWQHWITTKDGQCGSPLVSIIDGNILGIHSLTHTTNGSNYFVEFPEKFVATYLDAADGWCKNWKFNADKISWGSFILWEDAPEDFMSG**LVPRGVG**REYVRFAPGSTHHHHHH

HCV^{TVMV}-AI-FRB. SMSTSGSGSGSAKGSVVIVGRINLSGDTAYSQQTRGAAGIAATSATGRDKNQVDGEVQVLSTATQSFLATCVNGVCWTVYHGAGSKTLAGPKGPITQMYTNVDQDLVGWPAPPGARSMTPCTCGSSDLYLVTRHADVIPVRRRGDSRGSLLSPRPVSYLKGSSGGPLLCPSGHVVGIFRAAVCTRGVAKAVDFIPVESMETTMRGGSGGSGGSGG**ETVRFQS**GGSGGDELILCPLDLGGSGGSGGSGGSGGSGG**VAILWHEMWHEGLEEASRLYFGERNVKGMFEVLEPLHAMMERGPQTLKETSFNQAYGRDLMEAQEWCRKYMKSGNVKDLTQAWDLYYHVFRRI**GGTGHHHHHH

Library Screening.

Bacterial growth media and protease assay buffers. E. coli was grown in shaking incubator (Infors HT Multitron) at the rpm as indicated. Minimal autoinduction medium contained 0.5% glycerol, 0.05% glucose, 0.2% lactose, 50 mM KH_2PO_4, 50 mM Na_2HPO_4, 10 mM $(NH_4)_2SO_4$, $MgSO_4$, and 1× trace metal solution (6). Autolysis medium consisted of autoinduction medium supplemented with 200 ng/mL anhydro-tetracycline, but no trace metals. Protease assay buffer consisted of 50 mM Tris·HCl, 1 mM DTT, and 0.5 mM EDTA, pH 8.0. TVMV substrate solution was composed of protease assay buffer supplemented with 40 μM of the quenched fluorescent peptide substrate for TVMV (Table S2).

Procedure. Libraries of autoinhibited TVMV mutants were transformed into chemically competent BL21(DE3)-RIL cells hosting the autolysis plasmid 05665 (Fig. S1*B*) and plated onto LB agar plates supplemented with 100 μg/mL carbenicillin, 50 μg/mL kanamycin, and 34 μg/mL chloramphenicol. Following overnight incubation at 37 °C, single colonies were inoculated into 96 deep-well plates filled with 1 mL minimal autoinduction medium supplemented with 100 μg/mL carbenicillin, 50 μg/mL kanamycin, and 34 μg/mL chloramphenicol. Cells were grown for 72 h at 30 °C at 320 rpm and typically reached OD values of ∼10. To lyse cells, 100-μL aliquots of cell cultures from half a 96-well-plate (48 samples) were diluted twofold into autolysis medium (100 μL) and incubated for 90 min at 30 °C with agitation at 200 rpm. Aliquots of cell lysates (10 μL) were transferred in duplicates into separate halves of a black 96-well plate (Corning) filled with protease assay buffer (140 μL). Half of the duplicates were supplemented with 1 U thrombin to cleave the linker connecting TVMV to its autoinhibition domain. The reaction was initiated by addition of 50 μL substrate solution, which gave rise to 10 μM TVMV substrate peptide in the final reaction. The reaction was monitored using in a plate reader (Biotek Synergy 4) by measuring the release of a quenched fluorophore (7-methoxycoumarinyl-4-acetyl) at 405 nm following excitation at 330 nm. The induction of TVMV protease activities was evaluated by comparing the time course of the reactions in the presence and absence of thrombin. The plasmids encoding for mutants with high induction ratios were subsequently isolated from single colonies and subjected to sequencing.

Engineering Artificially Autoinhibited TVMV Modules.

Primary design. To create a TVMV-based signal transducer, the N-terminal cleavage product ETVRFQ (separated by a thrombin cleavage site flanked by additional glycine and serine residues) was appended to the C-terminal end of TVMV: ...GSFTLVEDAPEDDFMSG**LVPRGV**GRETVRFQ*.

Starting mutant: C-terminal tail of $TVMV^{WT}$ (underlined) and the N-terminal cleavage product (double underlined) acting as an AI-domain separated by a thrombin cleavage site (bold).

Library screen 1. To improve the performance of the TVMV-based module, the first library screen aimed to enhance the affinity between the product-based inhibitor and the TVMV protease through additional intercalating interactions between P5 and P6 in the N-terminal cleavage product and T214 and V216 in β13 of TVMV.

```
      W W                    W
      Y Y                   YY
      I I                   FF
...GSFTLVEDAPEDFMSGSG LVPRGV GRETVRFQ*
     4×4×                  3×4× = 192-fold Diversity
```

Library 1: C-terminal tail of TVMV (underlined) and the N-terminal cleavage product (double underlined) separated by a thrombin cleavage site (bold). The diversified amino acid positions are highlighted in red.

Library screen 2. The second library aimed to identify di-peptide motives that could bind across the P1-P1′ junction, but could not be cleaved by TVMV. In this way, it became possible to move the His_6 affinity purification tag from the N to the C terminus and enable purification of full-length proteins only. To this end, a small library with a proline in the P1′ position and a fully randomized P1 position was screened enabling us to identify a di-peptide motives covering the P1-P1′ junction that bound to the active site of TVMV but that were not cleaved. The design of the library was based on the notion that substrate mapping data for the related NIa protease from TEV suggests that proline in the P1′ position prevents cleavage (7). It is, however, unclear whether sequences with a proline in the P1′ position cannot bind or can bind but cannot be cleaved by TEV protease. Similarly, it is not clear to what extent this holds true for other members of the NIa potyvirus protease family including the NIa protease from TVMV.

```
...GSFILWEDAPEDFMSG LVPRGV GREYVRFXP GSTHHHHHH*
                                20× = 20-fold Diversity
```

Library 2: C-terminal tail of mutant $TVMV^{T214I,\ V216W}$ (underlined) and the AI domain (double underlined) separated by the thrombin cleavage site (bold). The diversified position X coding for all 20 amino acids and the proline residue in the P1′ position is highlighted in red.

Protein Expression and Purification.

Bacterial growth media and buffers. Terrific broth (TB) consisted of 1.2% (wt/vol) tryptone, 2.4% (wt/vol) yeast extract, 0.04% glycerol, 0.17 M KH_2PO_4, and 0.72 M K_2HPO_4. PBS consisted of 10 mM Na_2HPO_4, 2 mM KH_2PO_4, 137 mM NaCl, and 2.7 mM KCl, pH 7.4. Washing and binding buffer consisted of 20 mM Na_2HPO_4 and 20 mM imidazole, pH 8.0, which was supplemented with 300 mM NaCl for TVMV-based signal transducers, 500 mM NaCl for HCV-based signal transducers, and 1 M NaCl for TVMV-based affinity clamp receptors. Elution buffer was composed as washing and binding buffer except that it contained 500 mM rather than 20 mM imidazole. Protein storage buffer contained 50 mM Tris·HCl and 10% (vol/vol) glycerol, pH 8.0, which was supplemented with 1 mM EDTA and 2 mM DTT for TVMV-based signal transducers, 1 M NaCl, 1 mM EDTA, and 2 mM DTT for TVMV-based allosteric receptors, and 500 mM NaCl and 2 mM β-mercaptoethanol for HCV-based signal transducers.

Protein expression. Plasmids were transformed into chemically competent BL21(DE3)-RIL cells and plated onto Luria Bertani (LB) agar plates supplemented with 100 μg/mL carbenicillin and 34 μg/mL chloramphenicol and incubated overnight at 37 °C. A single colony was used to inoculate TB medium (250 mL) supplemented with 0.2% lactose, 0.05% glucose, 2 mM $MgCl_2$, 100 μg/mL carbenicillin, and 34 μg/mL chloramphenicol. Cells were grown over the course of 48 h at 30 °C at 200 rpm and the protein expressed by autoinduction. Cells usually reached OD_{600} values of ∼14 before being harvested by centrifugation at 4,500 × *g*, washed once with PBS (500 mL), and stored at −20 °C.

Protein purification. To purify the protease-based signal transducers and allosteric receptors, cells were resuspended in washing and binding buffer and lysed using a one shot cell disruptor (Constant Systems). Samples were subsequently centrifuged at 25,000 × *g*, and the supernatant was passed through a 0.25-μm nitrocellulose filter. The His_6-tagged proteins were purified using the AKTA-Express FPLC system. Briefly, the lysate was loaded onto Ni-NTA columns (5 mL HisTrap FF Crude; GE Healthcare) equilibrated with the binding buffer, and the column was washed with 200 mL of the washing buffer. The protein was eluted with an imidazole gradient from 20 to 500 mM in 40-column volumes at a flow rate of 5 mL/min. The protein typically eluted around 100 mM imidazole. Fractions containing protein were subsequently pooled and concentrated with 10-kDa cutoff centrifugal filters (Amicon Ultra) and transferred into the storage buffer by gel filtration on disposable PD-10 desalting columns according to manufacturer's instructions (GE Healthcare). Proteins were generally stored at −80 °C.

Protease Assays.

Fluorogenic protease substrate peptides and affinity clamp peptide ligands. Protease substrates (Table S2) were obtained commercially (Mimotopes) and dissolved in DMSO to a final concentration of 8 mM and stored at −80 °C.

Assaying TVMV- and HCV-based signal transducers. To measure induction ratios under saturating reaction conditions, 500 nM TVMV- and HCV-based signal transducers were preincubated for 10 min in 150 μL protease assay buffer (50 mM Tris·HCl, 100 mM NaCl, 50 μg/mL BSA, and 2 mM DTT) in the presence and absence of the inducing protease: i.e., 1 U thrombin for TVMV-based signal transducers and 500 nM TVMV for HCV-based signal transducers. The reaction was initiated following the addition of 50 μL

substrate solution (Table S2) to a final concentration of 5 μM peptide substrate (Table S2) in a final reaction volume of 200 μL. The reaction was monitored using a fluorescent plate reader (Biotek Synergy 4) by measuring the release of 7-methoxycoumarinyl-4-acetyl from the quenched substrate peptide with $\lambda_{ex/em}$ of 330 and 405 nm. The induction ratio of TVMV-based protease activities in the inhibited and unhibited states was calculated by dividing the initial rate in the presence of the activating protease over the initial rate in the absence of the activating protease.

Enzyme kinetics of TVMV-based signal transducers. To determine the kinetic parameters, the proteolytic activity of different protease biosensors was measured in protease assay buffer over varying concentrations of the substrate TVMV-DD (Table S2) using the protease concentrations indicated in the figure captions. Measurements were performed in duplicate for each substrate concentration. Initial rates were extracted from the change in fluorescence (after subtracting the background fluorescence with no enzyme) and plotted against the substrate concentration. Kinetic parameters were subsequently obtained by a nonlinear regression fit of the curve to Eq. **S1**

$$Y = V_{\max} \times \frac{[\text{Substrate}]}{[\text{Substrate}] + K_M}. \qquad \textbf{[S1]}$$

To estimate the K_i of the inhibitory peptide EYVRFAP, 500 nM of the TVMV$^{\text{T214I, V216W}}$ mutant was assayed with 5 μM of the TVMV-DD substrate in the presence of varying concentrations of the inhibitory peptide EYVRFAPGST. Measurements were performed in duplicate for each inhibitor concentration, and the initial rates were extracted as described above. The K_i was subsequently determined by a nonlinear regression fit of the curve to Eq. **S2** with the K_M and the substrate concentration set to 65 and 5 μM, respectively

$$Y = V_{\max} \times \frac{[\text{Substrate}]}{[\text{Substrate}] + K_M \times \left(1 + \frac{[\text{Inhibitor}]}{K_i}\right)}. \qquad \textbf{[S2]}$$

Assaying TVMV-based allosteric receptors. The maximum induction ratios and apparent K_ds of TVMV-based allosteric receptors were measured in ligand titration experiments. The maximum induction ratios were measured using 250 nM TVMV affinity clamp chimera, whereas the apparent K_ds for the stronger and weaker binding affinity clamp ligands B1 and B2 were measured using 10 and 100 nM TVMV affinity clamp chimera, respectively. Initial rates were extracted from the change in fluorescence (after subtracting the background fluorescence with no enzyme) and plotted against the ligand concentration. The apparent K_ds of the different types of receptors were determined by a nonlinear regression fit of the curve to Eq. **S3**

$$Y = V_0 + (V_{\max} - V_0) \times \frac{([\text{Sensor}] + [\text{Ligand}] + K_d) - \sqrt{([\text{Sensor}] + [\text{Ligand}] + K_d)^2 - (4 \times [\text{Sensor}] \times [\text{Ligand}])}}{2 \times [\text{Sensor}]}. \qquad \textbf{[S3]}$$

Protease cascades. TVMV- and HCV-based signaling cascades were measured as described above except that the reaction was initiated by the addition of the HCV-based signal amplifier. The concentration of the two different ligands B1 and B2, the HCV-based signal transducers, and the TVMV-based allosteric receptors are indicated in the figure legends. The HCV-based substrate was included at 5 μM (Table S2). Initial rates were extracted from the change in fluorescence (after subtracting the background fluorescence with no enzyme) and plotted against the ligand concentration. The apparent K_ds were determined by a nonlinear regression fit of the curve to Eq. **S3**.

Protease-based proximity sensors. Protease-based proximity sensors tagged with FRB and FKBP were measured as described above except that the reaction was initiated by the addition of the FRB-tagged HCV-based signal amplifier. The concentration of rapamycin, the FRB-tagged HCV-based signal transducer, and the FKBP12-tagged TVMV-based signal transducer are indicated in the figure annotations. The HCV-based substrate was included at 5 μM (Table S2). Initial rates were extracted from the change in fluorescence (after subtracting the background fluorescence with no enzyme) and plotted against the concentration of rapamcyin. The apparent K_ds of for rapamycin was determined by a nonlinear regression fit of the curve to Eq. **S3**.

Rationale of Protease-Based Signal Transducers. In the simpler case of a protease-inducible transducer protease, we formulated a mathematical model based on Michaelis–Menten Kinetics defining the parameters modulating the signal output (Fig. S3). For any given autoinhibited transducer protease, the induction of activity is defined as the ratio of enzyme velocities in the cleaved and uncleaved states, which are subject to intra- and intermolecular inhibition, respectively, as defined by Eq. **S4**. Residual inhibition by the cleaved product peptides that remains associated with the protease is not taken into account in the model

$$\text{Induction} = \frac{V_{\text{Cleaved}}}{V_{\text{Uncleaved}}} = \frac{\frac{V_{\max} \times [S]}{K_M^{\text{Cleaved}} + [S]}}{\frac{V_{\max} \times [S]}{K_M^{\text{Uncleaved}} + [S]}}.$$

Assume competitive inhibition model

$$\text{Induction} = \frac{V_{\text{Cleaved}}}{V_{\text{Uncleaved}}} = \frac{\frac{V_{\max} \times [S]}{K_M\left(1 + \frac{[E]}{K_i}\right) + [S]}}{\frac{V_{\max} \times [S]}{K_M\left(1 + \frac{[I]}{K_i}\right) + [S]}}.$$

After cleavage $[I]^{\text{Cleaved}} = [E]$

$$\text{Induction} = \frac{V_{\text{Cleaved}}}{V_{\text{Uncleaved}}} = \frac{K_M\left(1 + \frac{[I]}{K_i}\right) + [S]}{K_M\left(1 + \frac{[E]}{K_i}\right) + [S]}.$$

Simplify

$$\text{Induction} = \frac{V_{\text{Cleaved}}}{V_{\text{Uncleaved}}} = \frac{1 + \frac{[I]}{K_i} + \frac{[S]}{K_M}}{1 + \frac{[E]}{K_i} + \frac{[S]}{K_M}}. \qquad \textbf{[S4]}$$

A plot of Eq. **S1** illustrates that the induction of activity is linearly proportional to the intramolecular concentration of the AI

domain in the uncleaved state [*I*] (Fig. S3). In practice, this effectively depends on the proximity of the N and C termini to the active site, as well as the structure and length of the connecting linker. The strength of binding of the AI domain K_i also favorably affects the induction ratio, but must not significantly exceed the operating concentration of the protease transducer to prevent continuing intermolecular inhibition after cleavage. Maximum induction is achieved under saturating reaction conditions at low substrate [*S*] and protease transducer concentrations [*E*] where competitive inhibition in the intra- and intermolecular states are minimized, and $[S] \ll K_M$ and $[E] \ll K_i$.

Note on Estimating Signal Amplification Factors. To obtain an estimate of signal amplification between the one- and two-stage systems, we estimate and compare signal amplification factors both in terms of absolute signal gain and in terms of signal-to-noise ratios. In the former case, protease signals were directly compared with each other, whereas in the latter case, protease signals were additionally normalized over the background signal in the absence of ligand (as denoted by the red traces in Fig. 3 *B* and *C*). Moreover, to estimate signal amplification factors, we compare the gradient in the exponential phase (Fig. S7 *A* and *C*) as an approximate estimation of increasing concentrations of active HCV, which can thus be more directly compared with the signal generated by TVMV in a single-stage setup. At the same time, we emphasize that it is difficult to compare signal amplification between first- and second-order processes based on one- and two-stage signal amplification systems. However, the fact that we obtain similar K_d values analyzing one- and two-stage amplification data indicates that the experimental setup and data analysis used are appropriate. Sequences for linkers L1, L2, and L3 encoding for different affinity clamp mutants are summarized in Table S1.

1. Nørholm MH (2010) A mutant Pfu DNA polymerase designed for advanced uracil-excision DNA engineering. *BMC Biotechnol* 10:21.
2. Villiers BR, Stein V, Hollfelder F (2010) USER friendly DNA recombination (USERec): a simple and flexible near homology-independent method for gene library construction. *Protein Eng Des Sel* 23(1):1–8.
3. Stein V, Hollfelder F (2009) An efficient method to assemble linear DNA templates for in vitro screening and selection systems. *Nucleic Acids Res* 37(18):e122.
4. Gibson DG, et al. (2009) Enzymatic assembly of DNA molecules up to several hundred kilobases. *Nat Methods* 6(5):343–345.
5. Kapust RB, et al. (2001) Tobacco etch virus protease: mechanism of autolysis and rational design of stable mutants with wild-type catalytic proficiency. *Protein Eng* 14(12): 993–1000.
6. Studier FW (2005) Protein production by auto-induction in high density shaking cultures. *Protein Expr Purif* 41(1):207–234.
7. Kapust RB, Tözsér J, Copeland TD, Waugh DS (2002) The P1′ specificity of tobacco etch virus protease. *Biochem Biophys Res Commun* 294(5):949–955.

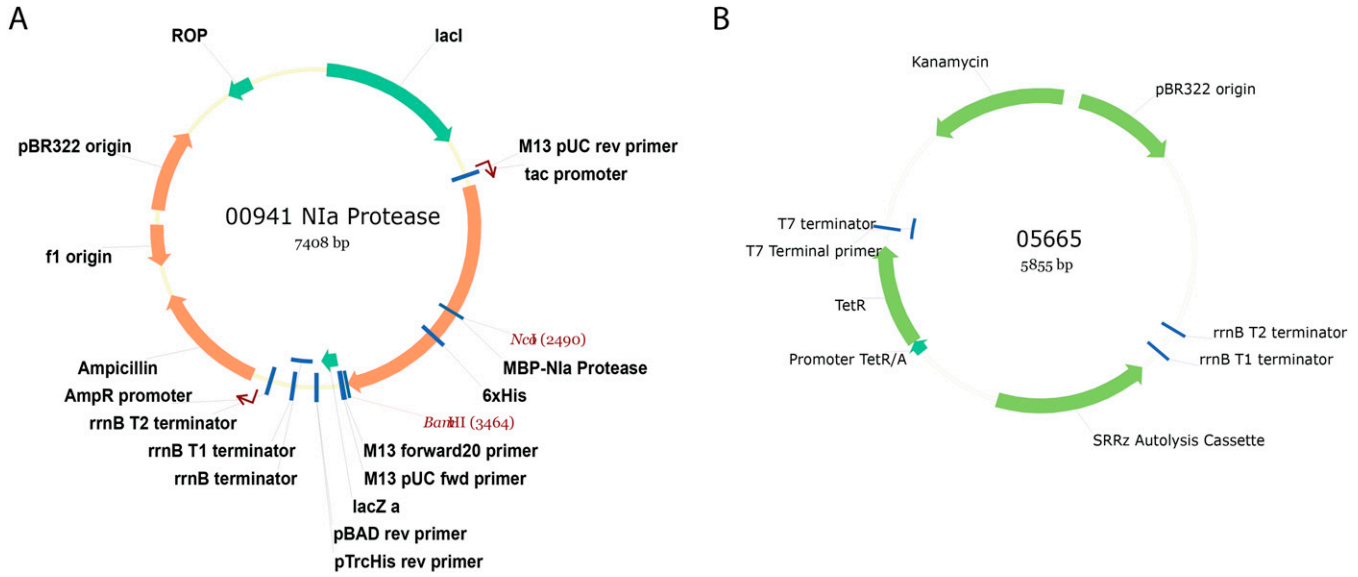

Fig. S1. (*A*) Plasmid map of the MBP-based expression vector 00941, which was used to express different fusion constructs of TVMV and HCV proteases. (*B*) Plasmid map of the autolysis vector 05665, which carries the λ-phage derived SRRz autolysis system under the control of the native, tetracycline-inducible bidirectional TetR/A promoter. The SRRz autolysis cassette includes its native 5′ UTR.

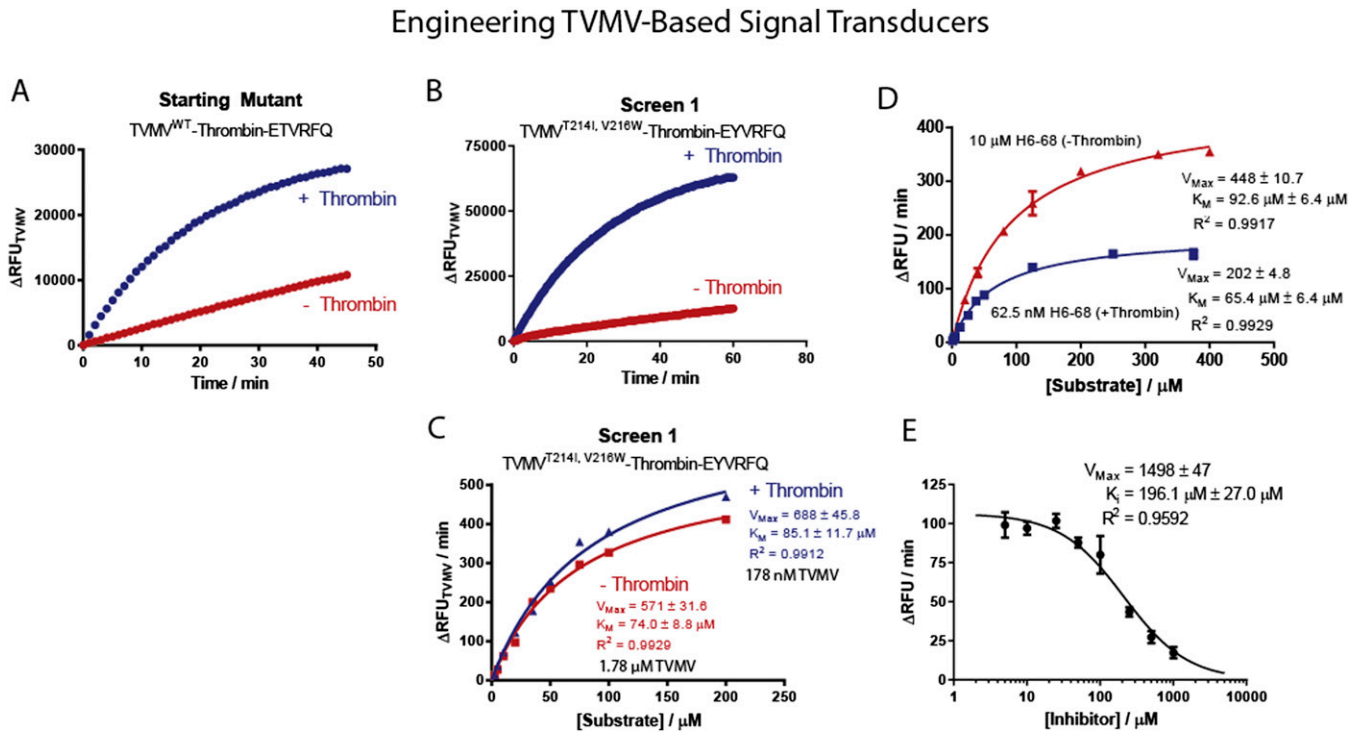

Fig. S2. Engineering TVMV-based signal transducers. (*A*) To create an artificially autoinhibited version of TVMV, its N-terminal cleavage product ETVRFQ was fused to its C terminus via a linker encoding a thrombin cleavage site, yielding a TVMV-based signal transducer (Starting Mutant), which activity could be induced by approximately fivefold following thrombin cleavage. Protease activities were measured using 892 nM TVMV and 5 μM TVMV substrate. (*B*) To improve the performance of the module, a library screen was devised to enhance the interactions affinity between TVMV and its AI domain. This screen yielded a mutant protease, $TVMV^{T214I,\ V216W}$, and an altered N-terminal cleavage product EYVRFQ serving as an AI domain (screen 1). Although the induction ratio improved slightly, to ∼13-fold, this was still considered insufficient for practical applications. Protease activities were measured using 892 nM TVMV and 10 μM TVMV substrate. (*C*) Notably, equivalent K_ms were determined for the TVMV-based protease activities before and after thrombin mediated activation, which suggests that the majority of background activity can be attributed to proteases that lack an AI domain as a result of premature termination of translation or proteolytic degradation. In the autoinhibited state, kinetic parameters were determined using 1.78 μM TVMV. In the activated state following thrombin cleavage, the kinetic parameters were determined using 178 nM TVMV. (*D*) Michaelis–Menten kinetics of mutant $TVMV^{V214I,\ T216W}$ in its activated (at 62.5 nM) and autoinhibited from (at 10 μM) assayed with varying concentrations of protease substrate TVMV-DD (Table S2). The kinetic parameters were determined by plotting the initial rates against the substrate concentration and the curve fit by nonlinear regression to Eq. **S1**. The K_m value for the thrombin activated form is in agreement with previously measured values for an equivalent substrate of WT TVMV using an HPLC-based assay (1). For the autoinhibited form, the K_m value associated with the residual activity is ∼70-fold weaker but still comparable to the uninhibited enzyme, indicating that this activity is still predominantly due to a population of uninhibited proteases. (*E*) Titration of 500 nM solution of the $TVMV^{T214I,\ V216W}$ mutant with increasing concentrations of the peptide derived from the autoinhibitor EYVRFAPGST. The K_i value was determined by plotting the initial rates against the ligand concentration and the curve fit by nonlinear regression to Eq. **S2**.

1. Sun P, Austin BP, Tözsér J, Waugh DS (2010) Structural determinants of tobacco vein mottling virus protease substrate specificity. *Protein Sci* 19(11):2240–2251.

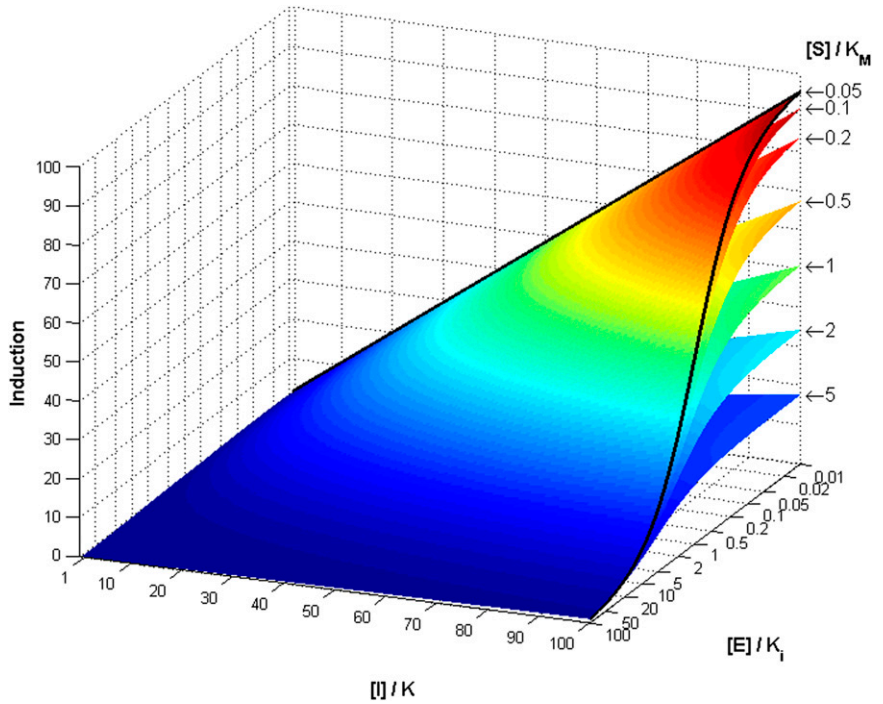

Fig. S3. Plot of the theoretical induction of activity of a protease-based signal transducer as a function of normalized substrate [S], enzyme [E], and effective, intramolecular concentration of the inhibitor [I] according to Eq. **S4**.

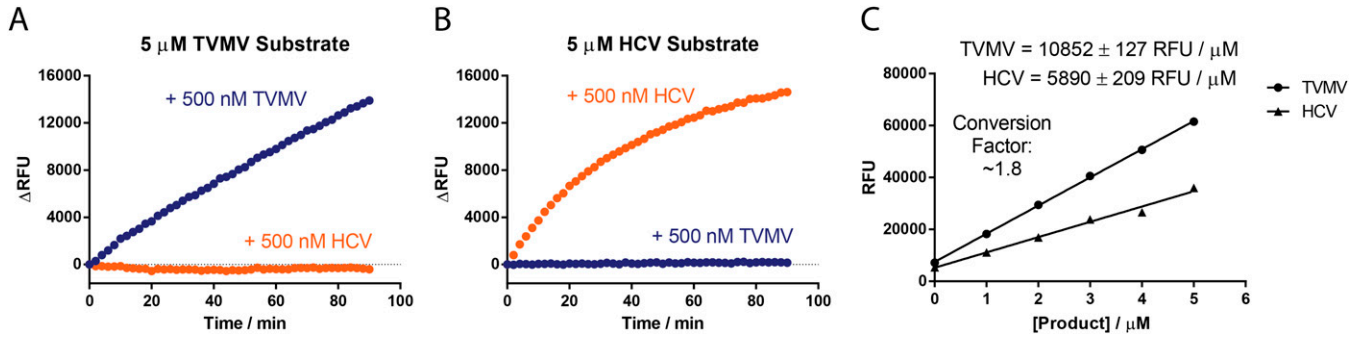

Fig. S4. TVMV- and HCV-based protease activities are mutually orthogonal. (*A*) TVMV$^{T214I,\ V216W}$ (at 500 nM) and HCV protease (at 500 nM) was incubated with TVMV substrate (at 5 μM). No appreciable cleavage of the TVMV substrate is achieved by HCV. (*B*) TVMV$^{T214I,\ V216W}$ (at 500 nM) and HCV protease (at 500 nM) were incubated with HCV substrate (at 5 μM). No appreciable cleavage is achieved by TVMV. (*C*) Comparison of RFUs generated by the cleavage of TVMV- and HCV-specific protease substrates. Over a range of 1–5 μM of cleaved protein substrates, RFUs are generated linearly for both TVMV- and HCV-specific cleavage products. RFU units generated through the cleavage of TVMV- and HCV-specific peptide protease substrates scale by a factor of 1.8.

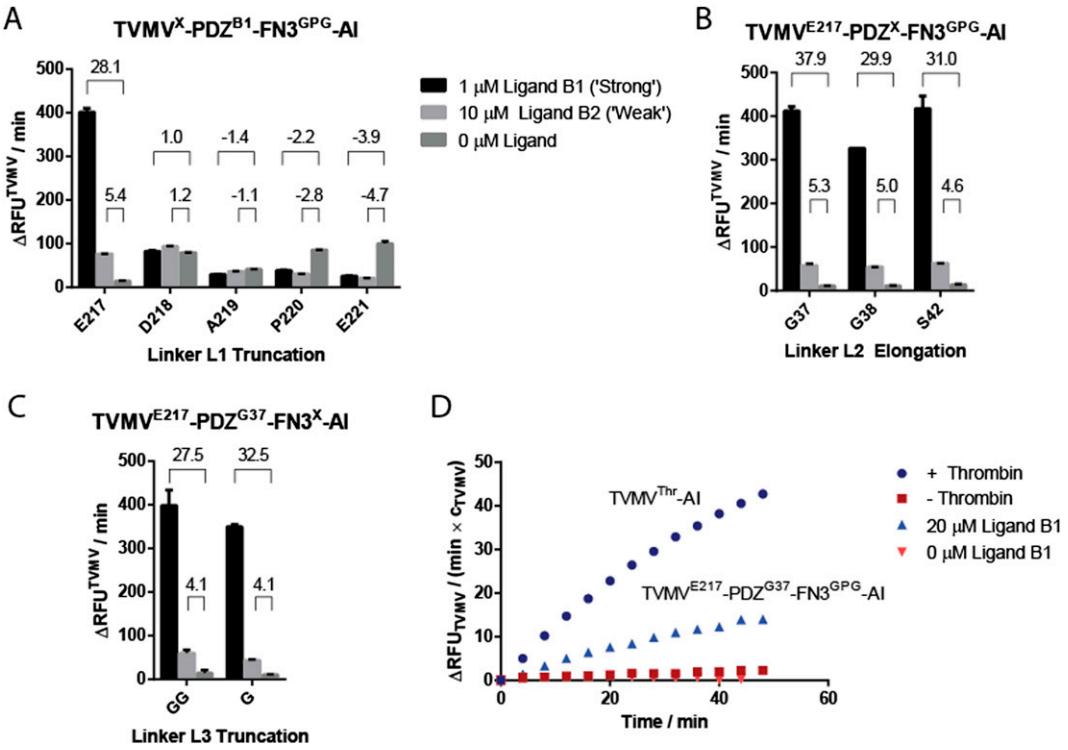

Fig. S5. Engineering TVMV-based ligand receptors. (*A*) The starting mutant TVMV^{E221}-PDZ^{G38}-FN3^{GPG}-AI responded to the addition of either ligand B1 or B2 in a switch-OFF fashion. Further shortening L1 by three amino acids yielded a ligand sensor TVMV^{D218}-PDZ^{B1}-FN3^{GPG}-AI that exhibited relatively low activities, but was largely unresponsive to the addition of either ligand B1 or B2. A single amino acid truncation then induced a sharp transition in the switching behavior yielding a ligand sensor TVMV^{E217}-PDZ^{B1}-FN3^{GPG}-AI that responded to the addition of the two different ligands B1 and B2 in 30- and 4-fold switch-ON fashions, respectively. (*B*) Elongation of linker L2 (connecting the PDZ domain with the FN3 domain) based on switch-ON mutant TVMV^{E217}-PDZ^{B1}-FN3^{GPG}-AI by a single glycine residue yielded mutant TVMV^{E217}-PDZ^{G37}-FN3^{GPG}-AI with a 37-fold induction ratio for ligand B2. Inserting up to four additional amino acids reduced the induction ratio down to 30-fold. (*C*) Further truncation of the GPG motif in linker L3 (connecting the FN3 domain with the AI domain) based on switch-ON mutant TVMV^{E217}-PDZ^{G37}-FN3^{GPG}-AI down to two or a single glycine residue did not appreciably alter the induction ratio. (*D*) Comparing the activities of TVMV-based signal transducer and TVMV-based allosteric protease receptor. Under full induction conditions, the TVMV-based allosteric protease receptor achieves 34% activity of the TVMV-based signal transducer (as judged by the concentration normalized initial rates over the first 12 min).

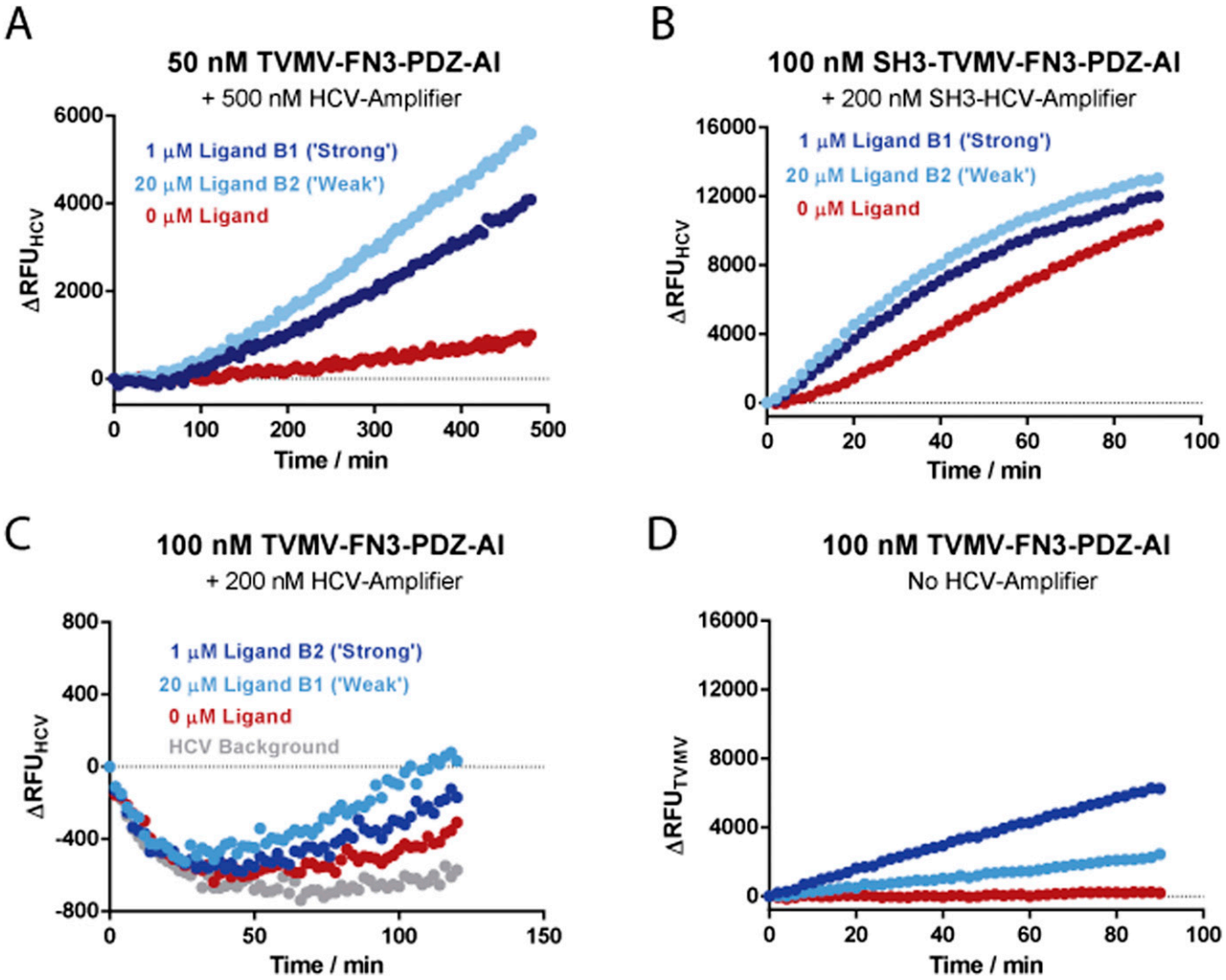

Fig. S6. Integrated signal sensing and signal amplification. (*A*) Signal transmission between a TVMV affinity clamp chimera and an HCV-based amplifier in the absence of scaffolding interactions. Time-resolved trace of HCV protease activities in signal sensing and amplification circuit based on a TVMV affinity clamp chimera (50 nM TVMV^{E217}-PDZ^{G38}-FN3^{GPG}-AI) and an HCV-based signal amplifier (500 nM HCV^{TVMV}-AI). Here, the TVMV-specific cleavage site in the HCV-based signal amplifier constitutes the only molecular recognition element that mediates signal transmission between the sensor and the amplifier. (*B*) Signal transmission between a TVMV affinity clamp chimera and an HCV-based amplifier in the presence of SH3-dependent scaffolding interactions based on an unscaffolded TVMV affinity clamp chimera (50 nM TVMV^{E217}-PDZ^{G38}-FN3^{GPG}-AI) and an HCV-based signal amplifier (500 nM HCV^{TVMV}-AI). (*C*) Comparing the time resolved traces of protease activities at high sensor concentrations in an integrated ligand sensing and amplification circuit based on an unscaffolded TVMV-based ligand sensor (100 nM TVMV^{E217}-PDZ^{G38}-FN3^{GPG}-AI) and an HCV-based signal amplifier (200 nM SH3-HCV^{TVMV}-AI) and (*D*) the TVMV-based ligand sensor (100 nM TVMV^{E217}-PDZ^{G38}-FN3^{GPG}-AI) on its own; here, scaffolding interactions are necessary for efficient signal transmission. RFU units generated through the cleavage of TVMV- and HCV-specific peptide protease substrates in the two different systems scale by a factor 1.8–1 (Fig. S4*C*).

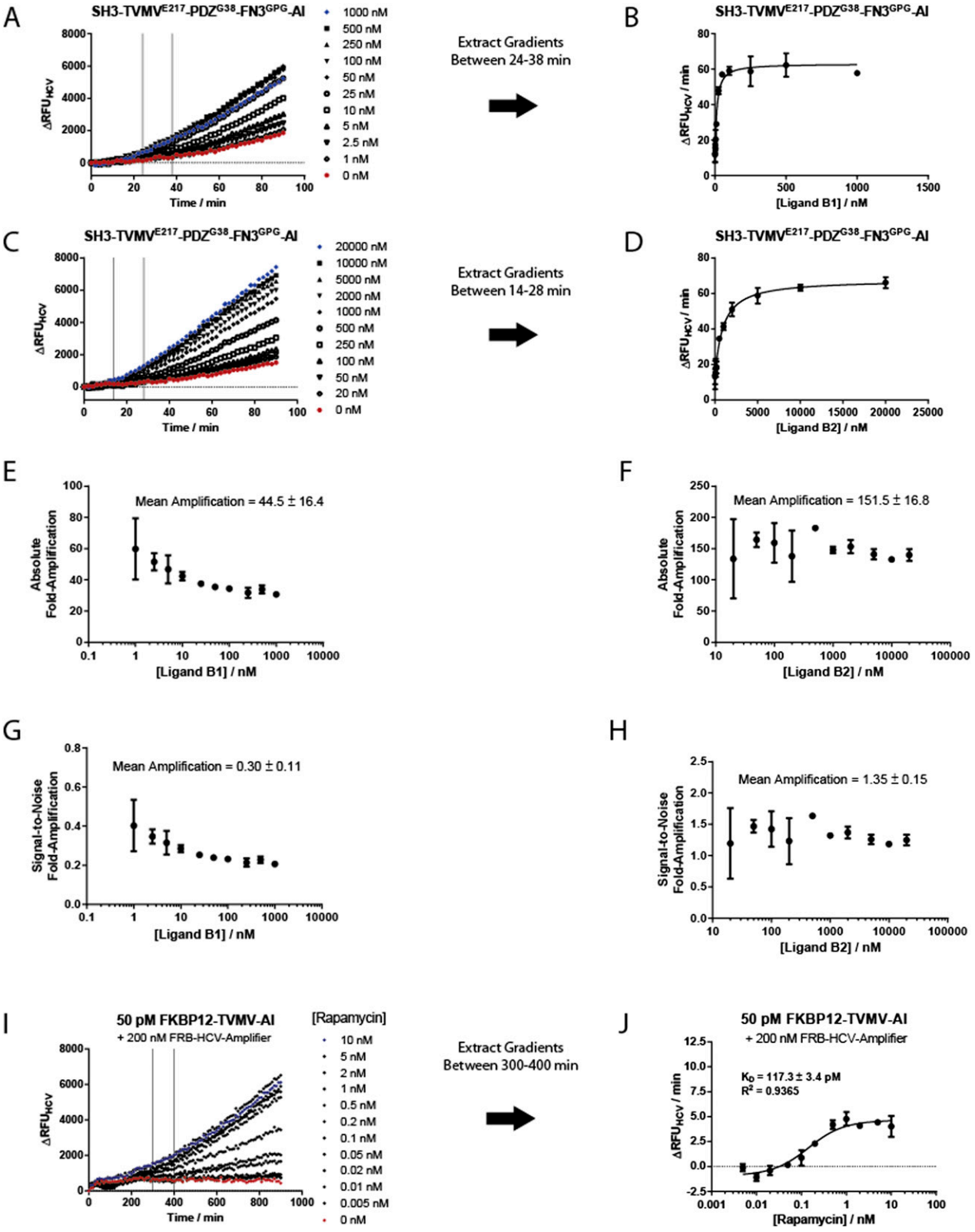

Fig. S7. Two-component signaling systems based on autoinhibited TVMV and HCV proteases. (*A–D*) Determination of the apparent K_ds in the two-stage amplification system. In the two-stage signal sensing and amplification system, the apparent K_ds of the receptor protease (SH3-TVMV^{E217}-PDZ^{G38}-FN3^{GPG}-AI) for ligands B1 and B2 were determined by plotting the observed change in fluorescence between (*A*) 24–38 min and (*C*) 14–28 min (as denoted by the vertical lines). The background fluorescence in the absence of enzyme was subtracted and the resulting values plotted against the ligand concentration and (*B* and *D*) fitted by the nonlinear regression to Eq. **S3**. Considering the irreversibility of HCV-based signal amplifier activation by the TVMV-based ligand sensor, the time window for recording the change in fluorescence was deliberately chosen before full activation of the HCV-based signal amplifier has occurred. (*E* and *F*)

Legend continued on following page

Determining amplification factors for absolute signals in the one- and two-stage amplification system across different concentrations of ligands B1 and B2: The concentration normalized change in fluorescence in the two-stage system (measured as HCV activity in the exponential phase) was divided by the change in fluorescence in the one stage system (measured through TVMV activity). (*G* and *H*) Determining amplification factors over signal-to-noise in the one- and two-stage amplification system across different concentrations of ligands B1 and B2: As in *E* and *F*, but this time the concentration normalized change in fluorescence for HCV- and TVMV-based signals was additionally normalized over the background signal for [Ligand] = 0 as derived from the curve fits in Fig. 3 *D* and *E*. (*I* and *J*) The apparent K_d for rapamycin binding to FKBP12:FRB in the two-component system using an autoinhibited TVMV transducer is comparable to the K_d obtained with uninhibited TVMV (Fig. 4*F*). To derive the apparent K_d the observed change in fluorescence between 300 and 400 min (as denoted on the plot by the vertical lines) was corrected for the background fluorescence in the absence of enzyme and plotted against the ligand concentration and the data were fitted by nonlinear regression to the Eq. **S3**.

Table S1. Summary of K_Ds for TVMV-based allosteric receptor proteases with switch-ON behavior

	Link sequences			Apparent K_Ds	
Mutant name	Linker L1	Linker L2	Linker L3	Ligand B1: RGSIDTWV (nM)	Ligand B2: PQPVDSWV (μM)
Receptor proteases with switch-OFF or neutral behavior (L1 truncations)					
$TVMV^{E217}$-PDZ^{E221}-$FN3^{GPG}$-AI	EDAPESG	GGSGG	GPG		
$TVMV^{E217}$-PDZ^{P220}-$FN3^{GPG}$-AI	EDAPSG	GGSGG	GPG		
$TVMV^{E217}$-PDZ^{A219}-$FN3^{GPG}$-AI	EDASG	GGSGG	GPG		
$TVMV^{E217}$-PDZ^{D218}-$FN3^{GPG}$-AI	EDSG	GGSGG	GPG		
Receptor proteases with switch-ON behavior (L2 elongation + L3 truncation)					
$TVMV^{E217}$-PDZ^{B1}-$FN3^{GPG}$-AI	ESG	GGSGG	GPG	11.9 ± 2.1	1.4 ± 0.2
$TVMV^{E217}$-PDZ^{G37}-$FN3^{GPG}$-AI	ESG	GGSGGG	GPG	11.4 ± 1.6	1.0 ± 0.1
$TVMV^{E217}$-PDZ^{G38}-$FN3^{GPG}$-AI	ESG	GGSGGGG	GPG	12.2 ± 2.1	1.3 ± 0.2
$TVMV^{E217}$-PDZ^{S42}-$FN3^{GPG}$-AI	ESG	GGSGGGGSGG	GPG	20.0 ± 2.0	2.9 ± 0.5
$TVMV^{E217}$-PDZ^{G37}-$FN3^{GG}$-AI	ESG	GGSGGGG	GG	15.7 ± 1.5	1.4 ± 0.2
$TVMV^{E217}$-PDZ^{G37}-$FN3^{G}$-AI	ESG	GGSGGGG	G	15.6 ± 1.5	1.2 ± 0.1
SH3-$TVMV^{E217}$-PDZ^{G38}-$FN3^{GPG}$-AI	ESG	GGSGGGGG	GPG	12.3 ± 1.6	1.3 ± 0.2
				10.0 ± 2.2	0.8 ± 0.2

Table S2. Summary of protease fluorogenic peptide substrates and peptide receptor ligands

Protease	Substrate sequence	Comments
TVMV	ANA-GETVRFQSDT(164)-NH_2	Used in library screening and protease activity assays
HCV	ANA-DDVTPCSMS(164)-NH_2	Used in library screening and protease activity assays
TVMV-DD	ANA-GETVRFQSDT(164)DD-NH_2	Used for measuring enzyme kinetics; contains additional Asp residues for improved water solubility
B1 ligand (strong)	NH_2-RGSIDTWV-COOH	K_d = 0.6 nM for the native affinity clamp ePDZ-b1
B2 ligand (weak)	NH_2-PQPVDSWV-COOH	K_d = 5 nM for the native affinity clamp ePDZ-b1

ANA, 5-amino-2-nitrobenzoyl group; 164, Mimotopes-specific code for lysine coupled to a 7-methoxycoumarinyl-4-acetyl group.